Journal of Membrane Science 652 (2022) 120467

Contents lists available at ScienceDirect

Journal of Membrane Science

journal homepage: www.elsevier.com/locate/memsci

Selective separation of HFC-32 from R-410A using poly(dimethylsiloxane) and a copolymer of perfluoro(butenyl vinyl ether) and perfluoro (2,2-dimethyl-1,3-dioxole)

Abby N. Harders [a], Erin R. Sturd [a], Julia E. Vallier [b], David R. Corbin [a], Whitney R. White [c], Christopher P. Junk [c], Mark B. Shiflett [a,*]

[a] University of Kansas, Institute for Sustainable Engineering, Lawrence, KS, 66045, USA
[b] Georgia Institute of Technology, Atlanta, GA, 30332, USA
[c] Chromis Technologies, Warren, NJ, 07059, USA

ARTICLE INFO

Keywords:
Perfluoropolymers
Refrigerant
Separation
PDMS
Membrane

ABSTRACT

Currently, millions of kilograms of HFCs and HFC mixtures are in use with no method for efficiently separating the components. Membranes are an attractive method for separating HFC refrigerant mixtures due to both lower energy consumption and capital requirements compared with alternative separation methods such as distillation. This study investigates the use of poly(dimethylsiloxane) and CyclAFlor™, an amorphous copolymer of 5 mol% perfluoro(butenyl vinyl ether) and 95 mol% perfluoro(2,2-dimethyl-1,3-dioxole), for the separation of R-410A, an azeotropic mixture composed of 50 wt% difluoromethane (HFC-32, CH_2F_2) and 50 wt% pentafluoroethane (HFC-125, CHF_2CF_3). Pure gas permeability of HFC-32 and HFC-125 were measured using a static membrane apparatus and the pressure-rise method. Solubility and diffusivity were measured using a gravimetric microbalance. Permeability measurements indicate high selectivity of HFC-32 over HFC-125 with CyclAFlor™, and mixed gas selectivity measurements utilizing a mixed gas apparatus are in excellent agreement with ideal selectivity calculations based on solubility and diffusivity measurements. Stability studies indicate that plasticization of the fluorinated amorphous polymer membrane is minimal in the presence of HFC-32 and HFC-125.

1. Introduction

Over recent years, legislation has been proposed for the eventual phase-out of hydrofluorocarbon refrigerants. Hydrofluorocarbons (HFCs) are a class of compounds widely used in refrigeration and air conditioning systems. These refrigerants were created to replace chlorofluorocarbon (CFC) and hydrochlorofluorocarbon (HCFC) refrigerants that are linked to the depletion of the Earth's ozone layer. Although HFC refrigerants have zero ozone-depletion potential, many HFCs and HFC mixtures have high global warming potentials (GWP) [1]. It is estimated that the refrigeration sector alone constituted 7.8% of global greenhouse gas emissions in 2014 [2]. The Kyoto Protocol—an international treaty that extends the 1992 United Nations Framework Convention on Climate Change—postulates targets for the reduction of greenhouse gases including HFCs [3]. Moreover, EU Regulation no. 517/2014 implements the reduction of up to two-thirds of the 2010 fluorinated greenhouse gas emissions by 2030 [4]. Most recently, the 2020 United States stimulus package passed in the wake of the COVID-19 pandemic includes provisions to reduce the production and importation of HFC refrigerants by 85% by 2035 and implements the international platform of the Kigali Amendment to prevent warming of up to 0.5 °C [5]. With international and national initiatives in place for restricting the use of high GWP HFCs, energy-efficient separation methods are needed in order to effectively dispose and recycle azeotropic refrigerant mixtures that will be phased out over the next two decades.

R-410A, a near azeotropic refrigerant mixture composed of 50 mass % HFC-32 (CH_2F_2) and 50 mass% HFC-125 (CHF_2CF_3) is used in a large number of commercial and residential air-conditioning applications [6]. R-410A was developed to replace HCFC-22 (chlorodifluoromethane, $CHClF_2$), which was banned for use in new equipment in 2010. With substantial amounts of HFCs circulating globally—1000 ktons of HFCs are estimated to be in global circulation—the question of how industries should handle the surplus of unused R-410A and HFC refrigerants is a timely issue complicated by the lack of industrially feasible separation

* Corresponding author.
E-mail address: mark.b.shiflett@ku.edu (M.B. Shiflett).

https://doi.org/10.1016/j.memsci.2022.120467
Received 31 December 2021; Received in revised form 13 March 2022; Accepted 14 March 2022
Available online 18 March 2022
0376-7388/© 2022 Elsevier B.V. All rights reserved.

methods for azeotropic mixtures [2]. Without the ability to recycle and separate R-410A into its constituent refrigerants, venting these high GWP gases will occur and lead to global temperature rise. Venting unused refrigerants is illegal; however, currently, there is little oversight to prevent this practice from occurring. High-temperature incineration is the only disposal method available and is expensive as well as energy intensive [2,7]. In the case of R-410A, the ability to separate this refrigerant mixture into its individual components is beneficial both environmentally and financially, as HFC-32 has the potential of being repurposed into next generation hydrofluorooloefin (HFO) refrigerant mixtures. A report by the European Committee maintained that a 40% reduction of global warming impact could be obtained if 60% of the global demand for replacing HCFC-22 and R-410A in current applications was met with propane and HFC-32. A further reduction of 20% of the global warming impact could be achieved if HFC-32/HFO blends were used instead of pure HFC-32 [8]. Thus, energy efficient separation methods are needed so lower GWP refrigerants like HFC-32 can be repurposed into low GWP HFO blends [9].

Membranes provide a promising and unique opportunity for the separation of HFC mixtures. Advantages of membrane separation in comparison with other methods such as distillation include low energy requirements, low operating cost, and the ability to utilize differences in chemical structure (rather than boiling point) to influence permeability and selectivity [10]. The number of applications using polymeric separations, such as hydrogen recovery and air separation, has grown substantially in recent years [11]. The use of polymeric membranes for the separation of partially-fluorinated molecules is an under-investigated topic; however, there are sources in the literature which explore the permeability of fluoro/hydrofluoro/hydrochlorofluoro-carbons. A number of different papers have reported permeability of fluorocarbons in poly(dimethylsiloxane) (PDMS) [12–14]. Merkel et *al*. investigated the sorption, diffusion, and permeation of a number of permanent gases, hydrocarbons and perfluorocarbons (PFCs) in PDMS [14]. These authors discovered that the permeability coefficients of the perfluorinated penetrants were an order of magnitude lower than their hydrocarbon counterparts and appreciably lower than those of the permanent gases primarily because of the relatively low PFC solubility in the hydrocarbon-based PDMS. Ruan et al. proposed coupling a multi-stage PDMS membrane unit to a cryogenic distillation column for the separation of HFC-23 (trifluoromethane, CHF_3) from vent gas in HCFC-22 synthesis, showing that HFC-23 could be purified up to 99.5 mol% in an economically feasible manner [7]. Polyimide (PI) polymers have also been investigated in the literature for fluorocarbon separations [15–17]. Ruan et al. explored improving tetrafluoroethylene (CF_2=CF_2) recovery in the synthesis of PTFE and avoiding the traditional acetone absorption method by coupling a PI membrane unit to distillation [18]. Although most sources focus on the separation of fluorocarbons from air or permanent gases, the separation of hydrofluorocarbon refrigerants HFC-32, HFC-134a (1,1,1,2-tetrafluoroethane, CH_2FCF_3), and HFO-1234yf (2,3,3,3-tetrafluoropropene, CH_2=$CFCF_3$) using varying compositions of poly(ether-*block*-amide) (PEBA) membranes was reported by Pardo et al. [19] Pardo showed that pure gas permeabilities through all PEBA membranes displayed the same trend, where HFC-32 had the highest permeability, followed by HFC-134a, and HFO-1234yf. Under mixed gas conditions, the permeability of the membranes for HFC-32/HFO-1234yf and HFC-32/HFC-134a remained nearly identical to the pure gas performance, indicating the promising potential of membrane separation technology for HFC/HFO mixtures. Additional studies of Pebax membranes by Pardo et al. have also been conducted with ionic liquid Pebax mixed matrix membranes [6,20]. These authors concluded that composite membranes with 40 wt% of 1-ethyl-3-methylimidazolium tetrafluoroborate ($[C_2C_1im][BF_4]$) and 1-ethyl-3-methylimidazolium thiocyanate ($[C_2C_1im][SCN]$) had the highest mechanical stability and best separation performance due to the ionic liquid reducing the permeability of the largest molecule (HFO-1234yf) and increasing the permeability of the smaller molecules (HFC-32 and HFC-134a) [20].

Although published examples of fluorocarbon separations using membranes are limited, recent advancements in the synthesis and production of amorphous perfluorinated polymers provide an opportunity for HCFC, HFC, and HFO separations. Fluorinated polymers are attractive for separation processes due to high chemical and thermal stability. Commonly used perfluorinated polymers include polytetrafluoroethylene (PTFE) and PTFE copolymers [21]. Additionally, amorphous perfluoropolymers are promising membrane materials for gas separations, as they combine the characteristic fluoropolymer traits of chemical and thermal stability, hydrophobicity, and oleophobicity with increased permeability and solvent solubility. This combination of traits also results in decreased tendencies to age and plasticize, which are common pitfalls to the industrial use of hydrocarbon polymer membranes in separation processes [22,23]. In order to continue the exploration of polymeric membranes for the separation of hydrofluorocarbons, the current study investigated the use of membranes for the separation of HFC-32 from R-410A. Sorption, diffusion, and permeability data are presented for HFC-32 and HFC-125 in 2 different membrane films: rubbery PDMS and a copolymer of perfluoro(butenyl vinyl ether) (PBVE) and perfluoro(2,2-dimethyl-1,3-dioxole) (PDD) sold under the name CyclAFlor™. The copolymer composition used in this work consists of 5 mol% PBVE and 95 mol% PDD (5% PBVE-*co*-95%PDD). Permeability data are reported at two different temperatures. Single component sorption data of HFC-32 and HFC-125 in PDMS and 5%PBVE-*co*-95%PDD measured using a gravimetric microbalance at 308.15 K and 323.15 K are also included in the study. Time-dependent behavior of the penetrant/polymer systems is modeled using the one-dimensional Fick's Law to obtain diffusion coefficients.

2. Materials and methods

2.1. Materials

HFC-125 (CAS# 354-33-6) and HFC-32 (CAS# 75-10-5) with a minimum purity of 99.9 wt% were supplied by the Chemours Company (Newark, DE). CO_2 (CAS# 124-38-9) with a minimum purity of 99.995 wt% was purchased from Matheson Tri Gas. The quick-setting epoxy glue was J-B Weld ClearWeld™ Quick-Setting Epoxy (SKU 50112). PDMS films were purchased from Interstate Specialty Products. Chromis Technologies supplied CyclAFlor™ films. Polymer densities are shown in Table 2. Physical property data of HFC-125 and HFC-32 were obtained from the National Institute of Standards and Technology (NIST) REFPROP V.10.0 database.

2.2. Experimental Methodology

2.2.1. Permeability

The separation of gas mixtures through polymeric membranes is a function of solubility and diffusivity as described by the solution-diffusion mechanism. The permeability coefficient, *P*, characterizes the flux of a permeate through a membrane with a pressure drop (Δp) and a thickness, δ [22]. The permeability of a gas using a variable pressure, constant volume membrane apparatus can be described by the following equation,

Table 1
Critical properties, dipole polarizability (Å^3) and dipole moments (D) of HFC-32 and HFC-125[a].

Penetrant	T_c (K)	P_c (MPa)	ρ_c (kg/m^3)	α(Å^3)	μ_g(D)
HFC-32	351.26	5.782	424.00	2.761	1.978
HFC-125	339.33	3.629	4571.30	4.623	1.563

[a] Critical property data and dipole moments are from Abbott et al. Polarizability values are from Abbott et al. and Gussoni et al. [24,25].

Table 2
Density of PDMS and 5%PBVE-*co*-95%PDD

Polymer	ρ (g/cm³)
PDMS	0.965
5%PBVE-*co*-95%PDD	1.70

$$P = \frac{-V_{DS}\delta}{ARTt} \cdot \ln\left(\frac{p_{US} - p_{DS}}{P_{US}}\right) \quad (1)$$

where R (m³ Pa mol⁻¹ K⁻¹) is the gas constant, T (K) is the absolute temperature, A (m²) is the area of the membrane, p_{DS} (Pa) is the downstream pressure, p_{US} (Pa) is the upstream pressure, and V_{DS} (m³) is the downstream volume. This equation is valid within a low limit of downstream pressure, where the increase in downstream pressure is linear with respect to time and less than 1% of the upstream pressure. In this equation, the downstream pressure is taken as 0 at $t = 0$.

The permeability apparatus was installed inside a chemical fume hood equipped with molecular sieve dryers (W.A. Hammond Drierite Company Ltd., L68 NP303) for the removal of H_2O. A vacuum/turbo pump (Pfeiffer HiCube 80 Eco, HiPace 80 Turbo Pump with TC 110, DN 63 ISO–K) was stationed in the fume hood for degassing the apparatus and samples at low vacuum (10^{-7} MPa) before permeability measurements. A temperature control system allowed for the heating and temperature measurement of the sample from 293.15 to 373.15 K (Cal Controls 3300 Series Temperature Controller).

The PDMS films were used as received. The 5%PBVE-*co*-95%PDD films were prepared by creating a layered structure composed of two 15 cm × 15 cm, 200 μm thick, Kapton® films between two 15 cm × 15 cm, mirror-polished plates of stainless steel. In between the Kapton® films was placed a circular shim that had 5 cm ID, 7 cm OD, and was 200 mm thick. 200–300 mg of polymer sample were placed inside the shim. The stacked assembly was placed between the heated platens (593.15 K) of a benchtop Carver hydraulic press and the lower platen was raised just until contact was achieved. The polymer was allowed to soften for 5 min, at which time the lower platen was raised up to maximum pressure. The heaters were turned off and the stack was allowed to slowly cool to ambient temperature over approximately 6 h. The pressure was relieved and the stack disassembled to give approximately a 200-μm thick bubble-free polymer film in the shape of a disk. Note this melt-press method can lead to permeability differences in comparison to polymers produced using a solvent evaporation method [26].

The static membrane apparatus measured the permeability of a gas through a polymeric film adhered to a brass disk. The brass disk had a hole of known area (1.28 cm²) in which a polymeric film of known thickness was adhered to using a quick-setting epoxy glue. The thickness of the polymeric film was measured with a digital micrometer (Starrett Digital IP67 Outside Micrometer, No. 796.1). When the apparatus was assembled, the brass disk with the adhered film sat on a sintered metal support disk. Underneath the sintered metal disk was the downstream side of the apparatus, which has a known volume that is used in the permeability equation. The volume of the downstream-side was measured by intruding the downstream-side with a liquid of known mass and density.

When running permeability measurements, the apparatus was put under vacuum (<10^{-3} MPa) for a minimum of 12 h. After the degassing was complete, the gas was introduced into the upstream side of the membrane apparatus and maintained at a constant pressure. A pressure transducer accurate to ±0.05% full-scale (FS) with output monitored by a LabView Data acquisition program was included on the upstream and downstream side of the membrane module. The gas was allowed to permeate through the film until the permeation reached a steady state. Eq. (1) was then used to calculate the steady-state permeance of the gas/polymer system. The ideal selectivity, which is the ratio of the pure gas permeability of HFC-32 and HFC-125, was calculated at both experimental temperatures.

In this study, the pure component permeabilities of difluoromethane (CH_2F_2) and pentafluoroethane (CHF_2CF_3) were measured in the PDMS and 5%PBVE-*co*-95%PDD polymers at approximately 0.2 MPa and two different temperatures. For experimental validation purposes, CO_2 permeability in PDMS was measured and compared to results reported by the manufacturer. Mixed gas selectivity for R-410A in the 5%PBVE-*co*-95%PDD polymer was also measured with a dynamic mixed gas permeability apparatus connected to a mass spectrometer (Hiden Isochema Ltd., IGA 003, Warrington, United Kingdom). With this operation, a membrane was mounted in a similar fashion as with the static membrane apparatus, and the same degassing procedure was followed. R-410A was flowed past the membrane at a constant rate and the downstream permeate was analyzed for composition via the mass spectrometer. A mixed gas selectivity, also sometimes referred to as the "true" gas selectivity, was calculated by taking the ratio of the mole fractions of HFC-32/HFC-125 over the ratio of the mole fractions in the permeate stream.

2.2.2. Sorption measurements

A gravimetric microbalance (Hiden Isochema Ltd., IGA 003, Warrington, United Kingdom) was used to measure gas absorption of HFC-32 and HFC-125 into the polymeric films. The gravimetric microbalance is capable of measuring changes in sample mass as a function of gas composition, temperature, or pressure and allows for the determination of kinetic parameters and sorption equilibrium [27]. The instrumental components and theory of the gravimetric microbalance have been described in detail in a previous reference; however, modifications to the procedure have been made [28]. A rectangular strip (4 cm × 1 cm) of polymer film (300 mg) was placed on a small copper hook and hung on a tungsten hang-down wire. The sample was degassed under vacuum (10^{-10} MPa) at the measurement temperature for approximately 24 h to remove any residual water content or volatile impurities. In order to establish thermodynamic equilibrium, each pressure point was completed with a minimum time requirement of 12 h. Stability of the balance as well as the kinetic sorption profile were measured by the HISorp software program. The microbalance can be operated in two different modes: static mode or dynamic mode. In static mode, gas is admitted away from the sample and the pressure is kept constant by the use of admit and exhaust valves. In dynamic mode, a continuous stream of gas flows past the sample, with the exhaust valve controlling the setpoint pressure [27]. For these experiments, the balance was operated in dynamic mode. A jacketed water bath was used to control sample temperature, and the sample and counterweight temperatures were measured with an in-situ K-type thermocouple with an uncertainty of ±0.1 K. The thermocouple was calibrated with a platinum resistance thermometer (Hart Scientific SPRT model 5699 and readout Hart Scientific Blackstack model 1560 with a SPRT module 2560) with an accuracy of ±0.005 K. The resolution of the IGA microbalance is 0.0001 mg for absorption and desorption measurements at a given temperature and pressure. The gas sorption data were corrected for buoyancy and volume expansion as described previously [27]. Sorption isotherms of HFC-125 and HFC-32 in PDMS and the 5%PBVE-*co*-95%PDD films were measured.

2.2.3. Solubility coefficient determination

From the sorption data of the permeating gases in the polymeric films, the solubility of each penetrant was calculated using the following equation:

$$S = \frac{C}{p} \quad (2)$$

where S is the solubility, C is the concentration, and p is the permeate pressure.

Using Eq. (2), the solubility of each penetrant in the respective films were plotted versus the pressure. The solubility coefficient, S^{∞}, which is

the solubility at infinite dilution, is defined as follows:

$$S^{\infty} = \lim_{p \to 0} \left(\frac{C}{p} \right) \approx \left(\frac{dC}{dp} \right)_{p=0} \quad (3)$$

where C is the equilibrium penetrant concentration at the pressure p. The solubility coefficient at infinite dilution is consistent with the definition of the Henry's Law constant, k_H:

$$C = k_H p \quad (4)$$

Henry's law can effectively be used to characterize the solubility of low-sorbing species in most rubbery polymer systems, since the pressure dependence on solubility tends to be negligible.

For glassy polymers, the Dual Model Sorption model is used to calculate gas solubility. The total gas absorbed is described by two terms: (1) sorption described by Henry's Law and (2) sorption described by the Langmuir model as shown in Eq. (5),

$$C = k_H p + \frac{C_H' b p}{1 + b p} \quad (5)$$

where C_H' is the Langmuir capacity constant and b is the Langmuir affinity constant.

2.2.4. Fickian diffusion

Since the permeability is a function of the solubility and the diffusivity, the time-dependent absorption data for HFC-32 and HFC-125 in the polymeric films were collected with the gravimetric microbalance at 308.15 K and 0.2 MPa. The diffusivity was modeled using Fick's Second Law of diffusion, as shown in Eq. (6):

$$\frac{dC}{dt} = D \frac{d^2 C}{dx^2} \quad (6)$$

The following assumptions were made to describe the system:

(1) The permeating species dissolves by a one-dimensional (horizontal) diffusion process
(2) A thin boundary layer exists at the interface between the permeating species and the polymeric film, where the saturation concentration is instantly established
(3) Interactions between the permeating species and the polymeric film are physical

Given these assumptions, the following boundary and initial conditions were applied to describe the system:

$$\text{IC: } t = 0,\ 0 < x < \delta, \text{ and } C = C_o \quad (7)$$

$$\text{BC1: } t > 0,\ x = 0, \text{ and } C = C_s \quad (8)$$

$$\text{BC2: } t > 0,\ x = \frac{\delta}{2}, \text{and} \frac{dC}{dx} = 0 \quad (9)$$

where C is the concentration of the permeating species in the polymeric material as a function of time, C_s is the saturation concentration, δ is the film thickness, x is the horizontal location, and D is the constant diffusion coefficient. Solving this initial boundary value problem using separation of variables yields the following solution:

$$C = C_s - \frac{2}{\pi}(C_0 - C_s) \sum_{n=1}^{\infty} \left(\frac{(-1)^n - 1}{n} e^{-\frac{D\pi^2 n^2 t}{L^2}} \sin\left(\frac{\pi n x}{L}\right) \right) \quad (10)$$

where L is the thickness of the sample. In order to obtain the average concentration across the polymeric film, Eq. (10) can be integrated from 0 to L and divided by L. The average concentration is then represented by Eq. (11):

$$C = C_s + \frac{2}{\pi^2}(C_0 - C_s) \sum_{n=1}^{\infty} \left(\frac{(-1)^n - 1}{n^2} e^{-\frac{D\pi^2 n^2 t}{L^2}} (\cos(n\pi) - 1) \right) \quad (11)$$

Although Eq. (11) contains an infinite summation term, the first 20 terms provide sufficient numerical precision. In order to predict the diffusion coefficient of a species into a polymeric material at a specific temperature and pressure, a non-linear regression was used to fit the diffusion model to experimental concentration. The best-fit parameters of the regression were used to determine the equilibrium concentration (C_s) and the diffusion coefficient (D). This analysis has been used to determine the diffusion coefficient of gaseous species in ionic liquids using the gravimetric method [9,27]. This model is consistent with diffusion analysis presented in Crank's Mathematics of Diffusion [29].

3. Results and discussion

3.1. Permeability results

3.1.1. Experimental validation

To establish confidence with the results produced by the static membrane apparatus, the permeability of CO_2 in the PDMS membrane was measured three times according to the procedure specified in the Experimental Methodology section. The permeability reported by Interstate Specialty Products was 2700 Barrer at ambient temperature. The permeability reported here is 2610 ± 20 Barrer at 298 K, showing that the results are in good agreement.

3.1.2. Permeability and ideal selectivity

Permeability results for HFC-32 and HFC-125 in PDMS and the 5% PBVE-*co*-95%PDD polymer can be found Table 3.

For the rubbery PDMS membrane, the HFC-32 and HFC-125 permeability is high and the selectivity is relatively low. Following the method demonstrated by Ruan et al., a selectivity prediction for HFC-32 and HFC-125 was made by correlating solubility selectivity (relative to nitrogen) to critical temperature and diffusivity selectivity (relative to nitrogen) to critical volume for a number of different molecules, as shown in Fig. 1 [7].

The critical parameters for HFC-32 and HFC-125 can be found in Table 1. The selectivity of HFC-32/HFC-125 was calculated by locating the solubility and diffusivity selectivity of both gases from Fig. 1, taking the ratios of the two different selectivities and then multiplying them to obtain the overall selectivity of HFC-32/HFC-125. Using this analysis, the predicted selectivity is 3.93, which agrees well with the measured selectivity of 3.32 at 323.15 K and 3.41 at 308.15 K. In the predicted selectivity of HFC-32/HFC-125, the diffusivity selectivity outweighed that of the solubility selectivity. By characterizing the solubility effects in terms of the critical temperature, which is a representation of the condensability of the molecule, and the size effects in terms of the critical volume, it follows that the critical volume of HFC-125 is nearly double that of HFC-32, while their critical temperatures are within 12 K of each other. Further analysis of the diffusivity and solubility will be discussed in subsequent sections; however, the high permeance of HFC-

Table 3
Permeability and ideal selectivity of HFC-125 and HFC-32 at 0.2 MPa.

PDMS			
T(K)	*P* (Barrer) of HFC-32	*P* (Barrer) of HFC-125	α_{ideal}
308.15	2700 ± 10	792 ± 4	3.4 ± 0.1
323.15	2480 ± 30	748 ± 7	3.3 ± 0.1
5%PBVE-*co*-95%PDD			
T(K)	*P* (Barrer) of HFC-32	*P* (Barrer) of HFC-125	α_{ideal}
308.15	361 ± 2	30 ± 0.8	12.0 ± 0.3
338.15	550 ± 10	43.4 ± 0.3	12.7 ± 0.2

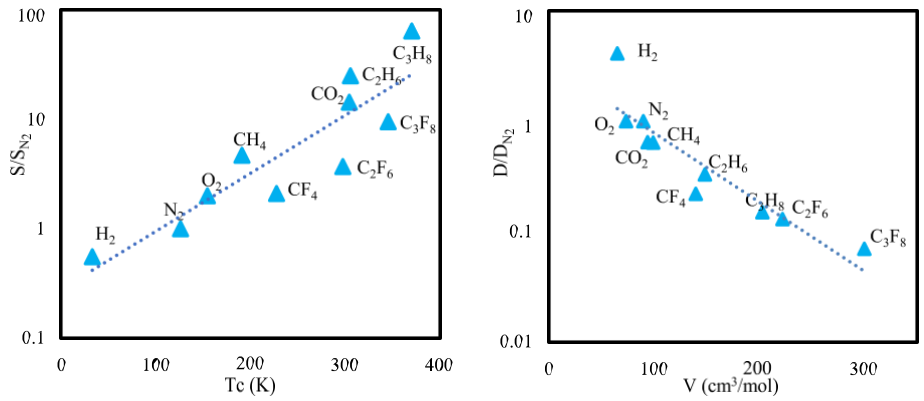

Fig. 1. Relative solubility selectivity as a function of critical temperature and relative diffusivity selectivity as a function of critical volume in PDMS [14].

32 correlates to its smaller size, and therefore to a higher diffusivity than the larger HFC-125. Fig. 2 shows a plot of the permeability of various gases in 5%PBVE-*co*-95%PDD and PDMS versus the critical volume. There is an overall decrease in the permeability with an increase in the critical volume indicating that the permeability is a strong function of the diffusivity. The H_2 and N_2 permeability in 5%PBVE-*co*-95%PDD agree with the reported trends in Okazy et al. at similar compositions [30]. The permeability of N_2 reported in the PDD homopolymer [31] was approximately 830 Barrer compared with the permeability of 700 Barrer in the 5%PBVE-*co*-95%PDD as shown in Fig. 2. The CO_2 permeability in a 50%PBVE-*co*-50%PDD polymer is reported in the literature to be approximately 200 Barrer. The permeability for CO_2 in the 5% PBVE-*co*-95%PDD polymer is predicted to be approximately 500 Barrer as shown in Fig. 2 [30]. The increase in CO_2 permeability is due to the increase in the PDD content in the copolymer.

For the 5%PBVE-*co*-95%PDD membrane, the permeability is lower for both HFC-32 and HFC-125 compared to the results in PDMS. The order of magnitude difference in permeability can be explained by the difference in polymer structures between PDMS and 5%PBVE-*co*-95% PDD. The rubbery nature of PDMS allows for flexible chain movements that can be characterized by its low density of 0.965 g/cm^3 and its low glass transition temperature of approximately 148.15 K [33]. For the 5% PBVE-*co*-95%PDD membrane, the density is 1.7 g/cm^3 and the glass transition temperature is approximately 524.15 K. The higher density and lower chain mobility of the 5%PBVE-*co*-95%PDD likely reduces the polymer free volume leading to lower gas permeability compared with PDMS. Moreover, it is hypothesized that the lower free volume of the 5% PBVE-*co*-95%PDD membrane leads to a higher selectivity of HFC-32 over HFC-125 due to the lower diffusion of HFC-125 through the polymer. The higher diffusivity in the PDMS overcomes the less favorable interactions between the HFCs and the hydrocarbon-based polymer compared with the more favorable interactions between the HFCs and the fluorinated 5%PBVE-*co*-95%PDD. Although the permeability is lower in 5%PBVE-*co*-95%PDD compared to PDMS, the permeability of gases through amorphous perfluorinated membranes is high in comparison to commercially available highly crystalline perfluoropolymers such as polytetrafluoroethylene (PTFE) [21,30].

Given the high selectivity of HFC-32/HFC-125 with 5%PBVE-*co*-95% PDD, the mixed gas selectivity was investigated. A stable and high mixed gas selectivity is imperative to showcasing the industrial feasibility of a membrane. The mixed gas selectivity of HFC-32/HFC-125 in 5%PBVE-*co*-95%PDD was determined to be 13.9 ± 0.8, which is in excellent agreement with calculated ideal selectivity. The selectivity as a function of time is shown in Fig. 3. The selectivity decreased during the first 5 h, but remained constant for the next 60 h. The initial change in selectivity may be due to the time required to reach steady-state.

3.2. Solubility results

Solubility isotherms for HFC-32 and HFC-125 at 308.15 K and 323.15 K in PDMS and 5%PBVE-*co*-95%PDD are shown in Fig. 4 and the Supplemental Information in Tables S1 and S2.

For PDMS and 5%PBVE-*co*-95%PDD polymers, the solubility of both HFC-32 and HFC-125 decreases with increasing temperature. This makes physical sense, as an increase in kinetic energy allows the gaseous molecules to escape sorption into the polymeric matrix. The solubility of HFC-32 and HFC-125 at 0.2 MPa in the two polymeric films are shown in Table 4. The solubility coefficients of HFC-32 and HFC-125 are significantly larger in the 5%PBVE-*co*-95%PDD film than in PDMS. The lower solubility of fluorinated compounds in PDMS agrees with other

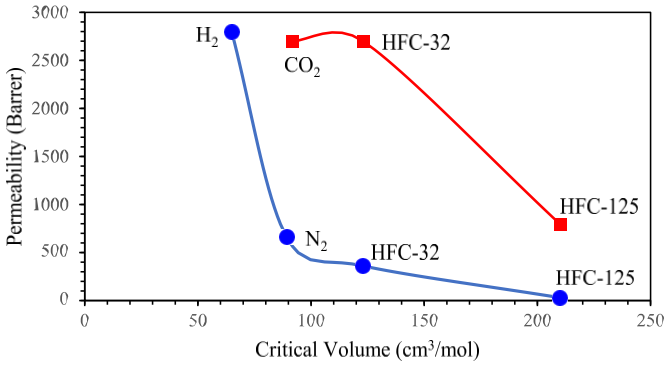

Fig. 2. Permeability as a function of penetrant size in 5%PBVE-*co*-95%PDD (●) and PDMS (■) at 308.15 K. Critical volume measurements were reported from literature [24,32].

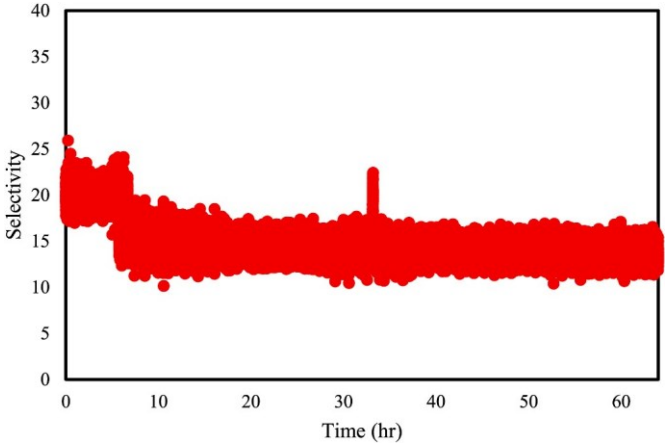

Fig. 3. Mixed gas selectivity of HFC-32/HFC-125 in 5%PBVE-*co*-95%PDD at 308.15 K.

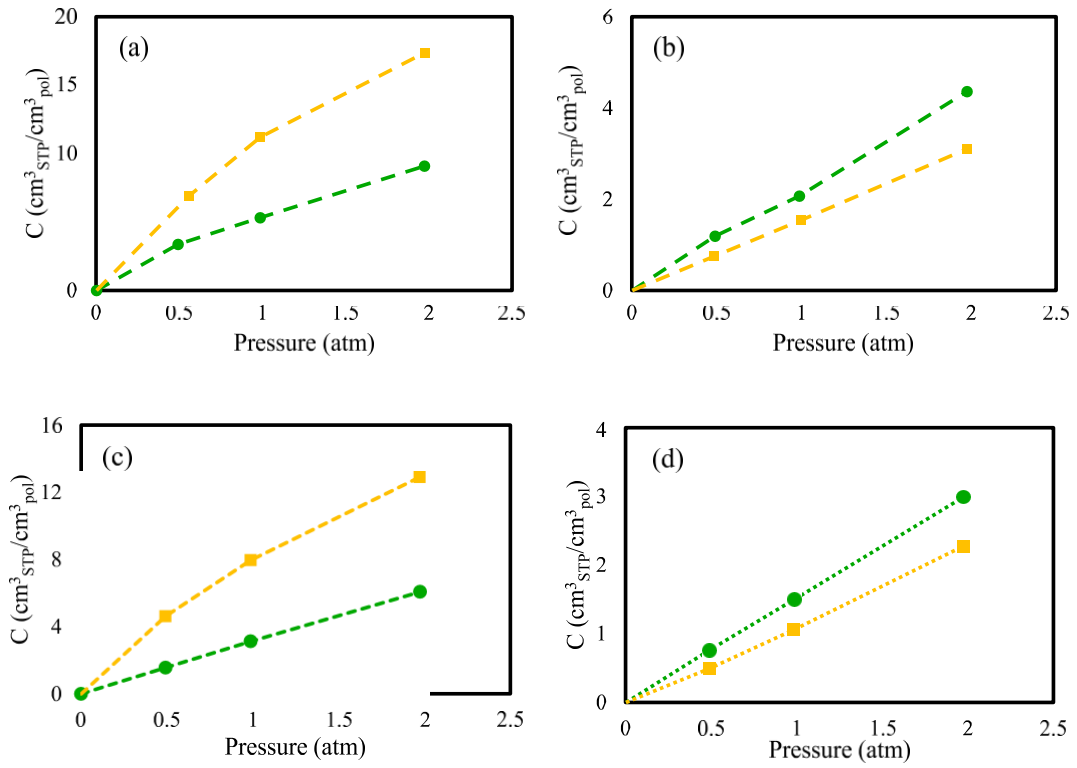

Fig. 4. Solubility isotherms of HFC-32 (●) and HFC-125 (■) in (a) 5%PBVE-*co*-95%PDD at 308.15 K (b) PDMS at 308.15 K (c) 5%PBVE-*co*-95%PDD at 323.15 K and (d) PDMS at 323.15 K.

Table 4
Solubility coefficients, diffusivity, and permeability result summary at 308.15 K and 0.2 MPa.

Solubility and Diffusivity of HFC-32 and HFC-125 in PDMS				
Penetrant	*S*	*D*	P_{calc}	P_{meas}
	(cm^3_{STP} /cm^3_{pol} ·atm)	(10^{-6} cm^2/s)	(Barrer)	(Barrer)
HFC-32	2.21 ± 0.03	9.2 ± 0.1	2670 ± 50	2700 ± 10
HFC-125	1.57 ± 0.04	3.8 ± 0.1	790 ± 30	792 ± 4
Solubility and Diffusivity of HFC-32 and HFC-125 in 5%PBVE-*co*-95%PDD				
Penetrant	*S*	*D*	P_{calc}	P_{meas}
	(cm^3_{STP} /cm^3_{pol} ·atm)	(10^{-6} cm^2/s)	(Barrer)	(Barrer)
HFC-32	4.61 ± 0.06	0.65 ± 0.1	390 ± 60	361 ± 2
HFC-125	8.80 ± 0.05	0.032 ± 0.01	38 ± 10	30 ± 0.8

solubility measurements in the literature. For example, the solubility of perfluoroethane (C_2F_6) in PDMS is 7.5 times lower than ethane, its hydrocarbon counterpart [14]. The low solubility of perfluorocarbons in PDMS can be ascribed to the fluorinated molecules unfavorable interactions with the hydrocarbon-based PDMS matrix in comparison to the 5%PBVE-*co*-95%PDD fluorinated matrix. The solubility of methane in PDMS has been reported in the literature as 0.42 ± 0.01 cm^3(STP)/cm^3·atm, and this work measured the solubility of HFC-32 in PDMS as 2.21 cm^3(STP)/cm^3·atm [14]. This much larger solubility for a perfluorinated compound may be due to dipole-dipole interactions that can occur between oxygen atoms in the PDMS and the polarized hydrogens in HFC-32 molecules. For the case of HFC-125 in PDMS, the solubility decreases in comparison to HFC-32. The solubility of ethane (C_2H_6) in PDMS is reported in the literature as 2.2 ± 0.02 cm^3(STP)/cm^3·atm, which is greater than the measured value of 1.57 cm^3(STP)/cm^3·atm for HFC-125 in this work [14]. In comparison to HFC-32, the single hydrogen of HFC-125 is less polarized and the molecule has a smaller dipole moment, thus contributing to a lower solubility of HFC-125 in PDMS. Using Henry's Law, the solubility values of HFC-125 and HFC-32 in PDMS at 0.2 MPa are 2.17 cm^3(STP)/cm^3·atm and 1.57 cm^3(STP)/cm^3·atm, respectively. The predicted solubility agrees well with the experimentally measured solubility.

The increased solubility of HFC-32 and HFC-125 in 5%PBVE-*co*-95% PDD relative to the solubility in PDMS can be attributed to the HFCs more favorable interactions with the fluorinated 5%PBVE-*co*-95%PDD. Amorphous perfluoropolymers have been shown to resist plasticization by condensable hydrocarbons due to repulsive forces existing between the hydrocarbon and the perfluorinated polymer [21]. For example, propane solubility in the homopolymer of PBVE and 2,2-bis(3,4-dicarboxyphenyl)hexafluoropropane dianhydride (6FDA) polyimide is 6.4 and 30 cm^3(STP)/cm^3 at 0.3 atm respectively, indicating largely unfavorable interactions of the non-fluorinated propane molecule in the fluorinated polymer [34]. In this study, the solubility of HFC-125 in 5% PBVE-*co*-95%PDD polymer is larger than HFC-32 at both 308.15 K and 323.15 K. This difference may be attributed to HFC-125 having a larger polarizability (4.36 Å^3) than HFC-32 (2.56 Å^3) and a higher fluorine-to-hydrogen ratio that leads to a greater strength of interaction with 5%PBVE-*co*-95%PDD [24]. Similar behavior has been demonstrated in the literature in regards to high-charge density ionic liquids, where the more polarizable molecules exhibit larger solubility [35]. It should also be noted that the behavior shown in Fig. 4 for rubbery PDMS and the glassy 5%PBVE-*co*-95%PDD agrees with sorption behavior reported in the literature, where the sorption in PDMS is in agreement with Henry's Law and the sorption in 5%PBVE-*co*-95%PDD is in agreement with the Dual Mode Sorption Law [36]. The solubility of HFC-125 and HFC-32 in 5%PBVE-*co*-95%PDD at 0.2 MPa was predicted by fitting the experimental data to the Dual Mode Sorption Model. The predicted solubility values at 0.2 MPa are 4.59 cm^3(STP)/cm^3·atm and 8.86 cm^3(STP)/cm^3·atm for HFC-32 and HFC-125, respectively. These results agree with the experimental solubility presented in Table 4; however, the uncertainties in the model parameters, specifically for HFC-125, are large due to the small number of experimental values that

were fit. Parameter estimates and solubilities at infinite dilution are reported in the supplementary information (see Table S3).

3.3. Fickian diffusion coefficients

The diffusion coefficients of HFC-32 and HFC-125 in PDMS and 5% PBVE-*co*-95%PDD are shown in Table 4. The diffusivity of HFC-32 is approximately 2.5 times greater than that of HFC-125 in PDMS and 20 times greater than HFC-125 in 5%PBVE-*co*-95%PDD. This larger difference in diffusivity between HFC-32 and HFC-125 in 5%PBVE-*co*-95% PDD is due to the more densely packed and less mobile polymer chains that may sterically hinder the diffusivity of HFC-125 more than that of HFC-32. In the PDMS membrane, the high chain mobility of the rubbery polymer provides little hindrance to the permeation of molecules based on differences in size, leading to diffusion coefficients of HFC-32 and HFC-125 that are of the same order of magnitude.

3.4. Measured permeability compared to permeability from physical properties

Table 4 gives two different permeability values: one that is measured with the static membrane apparatus and the other that is a function of the solubility and diffusivity. These two permeability values, which are measured independently of each other, are in exceptional agreement, indicating that the solution-diffusion mechanism accurately describes the transport of HFC-32 and HFC-125 in both PDMS and 5%PBVE-*co*-95%PDD. The selectivity in terms of the diffusivity, solubility and permeability is presented in Table 5. The diffusivity selectivity largely drives the selectivity of HFC-32 and HFC-125 in 5%PBVE-*co*-95%PDD. In terms of selectivity, the 5%PBVE-*co*-95%PDD polymer provides an opportunity to adjust the ratio of PBVE and PDD monomers in order to provide a more selective separation. The PDD monomer contains bulky CF_3 groups that contribute to a lower density and a higher fractional free volume as the percentage of PDD in the copolymer increases. Thus, adjusting the ratio of PDD and PBVE provides the opportunity to improve the selectivity based on a kinetic separation, albeit with a decrease in the copolymer's permeability as illustrated by the Robeson's bound tradeoff [37]. Although there are not many examples of polymers in the literature for the separation of HFC-32 and HFC-125, the selectivity of HFC-32/HFC-125 in Pebax 1657 was reported by Pardo et al. as approximately 7 [19]. Thus, the selectivity reported for HFC-32/HFC-125 of a neat polymeric membrane in this study is the highest known value in the literature to our knowledge, not taking into consideration mixed matrix membranes that have led to selectivities in the 20s.

4. Conclusions

The results of this study show that amorphous fluoropolymers provide an opportunity for the selective separation of HFC-32 from refrigerant mixtures such as R-410A. The selectivity achieved with the 5% PBVE-*co*-95%PDD membrane is approximately four times higher than the selectivity achieved with PDMS and is the highest selectivity known in the literature using polymeric membranes for HFC separations. Mixed gas selectivity is in excellent agreement with the ideal gas selectivity and remained stable for over 60 h indicating the resistance to plasticization. The solubility and diffusivity measurements indicate that the separation of HFC-32 from R-410A is largely a diffusivity-driven separation. This indicates that modifications in the composition of PBVE-*co*-PDD that decrease the fractional free volume could lead to membranes with even higher selectivity for HFC mixtures. Fluorinated membranes provide new materials for separating azeotropic refrigerant mixtures such as R-410A so that HFC-32 can be reused in low GWP HFO blends in the future.

Table 5
Selectivity based on the solubility, diffusivity, and permeability of HFC-32 and HFC-125 at 308.15 K

Polymer	$S_{HFC\text{-}32}/S_{HFC\text{-}125}$	$D_{HFC\text{-}32}/D_{HFC\text{-}125}$	$P_{HFC\text{-}32}/P_{HFC\text{-}125}$
PDMS	1.41 ± 0.04	2.4 ± 0.1	3.4 ± 0.1
5%PBVE-*co*-95%PDD	0.524 ± 0.007	20 ± 7	10 ± 3

Funding

This material is based upon work supported by the National Science Foundation under Grant No. 2029354.

Declaration of competing interest

The authors declare that they have no known competing financial interests or personal relationships that could have appeared to influence the work reported in this paper.

Acknowledgements

The authors acknowledge the University of Kansas Chancellor's Doctoral Fellowship for support of this research.

Appendix A. Supplementary data

Supplementary data to this article can be found online at https://doi.org/10.1016/j.memsci.2022.120467.

References

[1] H. Duan, T.R. Miller, G. Liu, X. Zeng, K. Yu, Q. Huang, J. Zuo, Y. Qin, J. Li, Chilling prospect: climate change effects of mismanaged refrigerants in China, Environ. Sci. Technol. 52 (2018) 6350–6356, https://doi.org/10.1021/acs.est.7b05987.
[2] D. Coulomb, C. Morlet, The Impact of the Refrigeration Sector on Climate Change, 35th Informatory Note on Refrigeration Technologies, IIF-IIR, 2017. https://iifiir.org/en/fridoc/the-impact-of-the-refrigeration-sector-on-climate-change-141135. (Accessed 14 June 2021).
[3] K. Simeonova, Kyoto Protocol Reference Manual on Accounting of Emissions and Assigned Amount, 2008, in: https://unfccc.int/process-and-meetings/the-kyoto-protocol/what-is-the-kyoto-protocol/kyoto-protocol-targets-for-the-first-commitment-period. (Accessed 11 January 2021).
[4] A. Mota-Babiloni, J. Navarro-Esbrí, Á. Barragán-Cervera, F. Molés, B. Peris, Analysis based on EU Regulation No 517/2014 of new HFC/HFO mixtures as alternatives of high GWP refrigerants in refrigeration and HVAC systems, Int. J. Refrig. 52 (2015) 21–31, https://doi.org/10.1016/j.ijrefrig.2014.12.021.
[5] EPA, Protecting Our Climate by Reducing Use of Hydrofluorocarbons Proposed Rule-Phasedown of Hydrofluorocarbons: Establishing the Allowance Allocation and Trading Program under the American Innovation and Manufacturing Act, 2021. https://www.epa.gov/climate-hfcs-reduction. (Accessed 22 July 2021).
[6] F. Pardo, G. Zarca, A. Urtiaga, Effect of feed pressure and long-term separation performance of Pebax-ionic liquid membranes for the recovery of difluoromethane (R32) from refrigerant mixture R410A, J. Membr. Sci. 618 (2021) 118744, https://doi.org/10.1016/j.memsci.2020.118744.
[7] X. Ruan, Y. Dai, L. Du, X. Yan, G. He, B. Li, Further separation of HFC-23 and HCFC-22 by coupling multi-stage PDMS membrane unit to cryogenic distillation, Separ. Purif. Technol. 156 (2015) 673–682, https://doi.org/10.1016/j.seppur.2015.10.064.
[8] B. Zeiger, B. Gschrey, Alternatives to HCFCs/HFCs in Unitary Air Conditioning Equipment at High Ambient Temperatures November 2014, 2014.
[9] A.R.C. Morais, A.N. Harders, K.R. Baca, G.M. Olsen, B.J. Befort, A.W. Dowling, E. J. Maginn, M.B. Shiflett, Phase equilibria, diffusivities, and equation of state modeling of HFC-32 and HFC-125 in imidazolium-based ionic liquids for the separation of R-410A, Ind. Eng. Chem. Res. 59 (2020) 18222–18235, https://doi.org/10.1021/acs.iecr.0c02820.
[10] R. Abedini, Application of membrane is gas separation processes: its sustainability and mechanisms, Petrol. Coal. 52 (2010) 69–80.
[11] D.F. Sanders, Z.P. Smith, R. Guo, L.M. Robeson, J.E. McGrath, D.R. Paul, B. D. Freeman, Energy-efficient polymeric gas separation membranes for a sustainable future: a review, Polymer 54 (2013) 4729–4761, https://doi.org/10.1016/j.polymer.2013.05.075.
[12] S.A. Stern, S.R. Sampat, S.S. Kulkarni, Tests of a "free-volume" model of gas permeation through polymer membranes. II. Pure Ar, SF6, CF4, and C2H2F2 in polyethylene, J. Polym. Sci. B Polym. Phys. 24 (1986) 2149–2166, https://doi.org/10.1002/POLB.1986.090241001.
[13] R.S. Prabhakar, T.C. Merkel, B.D. Freeman, T. Imizu, H. Akon, Sorption and transport properties of propane and perfluoropropane in poly(dimethylsiloxane)

and poly(1-trimethylsilyl-1-propyne), Macromolecules 38 (2005) 1899–1910, https://doi.org/10.1021/MA048032K.
[14] T.C. Merkel, V.I. Bondar, K. Nagai, B.D. Freeman, I. Pinnau, Gas sorption, diffusion, and permeation in poly(dimethylsiloxane), J. Polym. Sci. B Polym. Phys. 38 (2000) 415–434, https://doi.org/10.1002/(SICI)1099-0488, 20000201)38:3.
[15] Y.-E. Li, Separation of CF_4 and C_2F_6 from a Perfluorocompound Mixture, 1999, EP0950430A1.
[16] I.J. Chung, K.R. Lee, S.T. Hwang, Separation of CFC-12 from air by polyimide hollow-fiber membrane module, J. Membr. Sci. 105 (1995) 177–185, https://doi.org/10.1016/0376-7388(95)00058-K.
[17] J.G. Wijmans, Z. He, T.T. Su, R.W. Baker, I. Pinnau, Recovery of perfluoroethane from chemical vapor deposition operations in the semiconductor industry, Separ. Purif. Technol. 35 (2004) 203–213, https://doi.org/10.1016/S1383-5866(03)00142-4.
[18] X. Ruan, G. He, B. Li, J. Xiao, Y. Dai, Cleaner recovery of tetrafluoroethylene by coupling residue-recycled polyimide membrane unit to distillation, Separ. Purif. Technol. 124 (2014) 89–98, https://doi.org/10.1016/j.seppur.2014.01.014.
[19] F. Pardo, G. Zarca, A. Urtiaga, Separation of refrigerant gas mixtures containing R32, R134a, and R1234yf through poly(ether- block-amide) membranes, ACS Sustain. Chem. Eng. 8 (2020) 2548–2556, https://doi.org/10.1021/acssuschemeng.9b07195.
[20] F. Pardo, S.v. Guti´errez-Hern´andez, G. Zarca, A. Urtiaga, Toward the recycling of low-GWP hydrofluorocarbon/Hydrofluoroolefin refrigerant mixtures using composite ionic liquid–polymer membranes, ACS Sustain. Chem. Eng. 9 (2021) 7012–7021, https://doi.org/10.1021/acssuschemeng.1c00668.
[21] Y. Okamoto, H.C. Chiang, M. Fang, M. Galizia, T.C. Merkel, M. Yavari, H. Nguyen, H. Lin, Perfluorodioxolane polymers for gas separation membrane applications, Membranes 10 (2020) 1–14, https://doi.org/10.3390/membranes10120394.
[22] Y. Yampolskii, Polymeric gas separation membranes, Macromolecules 45 (2012) 3298–3311, https://doi.org/10.1021/ma300213b.
[23] Y. Yampolskii, N. Belov, A. Alentiev, Perfluorinated polymers as materials of membranes for gas and vapor separation, J. Membr. Sci. 598 (2020) 117779, https://doi.org/10.1016/J.MEMSCI.2019.117779.
[24] A.P. Abbott, C.A. Eardley, R. Tooth, Relative permittivity measurements of 1,1,1,2-tetrafluoroethane (HFC 134a), pentafluoroethane (HFC 125), and difluoromethane (HFC 32), J. Chem. Eng. Data 44 (1999) 112–115, https://doi.org/10.1021/je980130b.
[25] M. Gussoni, M. Rui, G. Zerbi, Electronic and relaxation contribution to linear molecular polarizability. An analysis of the experimental values, J. Mol. Struct. 447 (1998) 163–215, https://doi.org/10.1016/S0022-2860(97)00292-5.
[26] M. Macchione, J.C. Jansen, G. de Luca, E. Tocci, M. Longeri, E. Drioli, Experimental analysis and simulation of the gas transport in dense Hyflon® AD60X membranes: influence of residual solvent, Polymer 48 (2007) 2619–2635, https://doi.org/10.1016/J.POLYMER.2007.02.068.
[27] M.B. Shiflett, A. Yokozeki, Solubilities and diffusivities of carbon dioxide in ionic liquids: [bmim][PF6] and [bmim][BF4], Ind. Eng. Chem. Res. 44 (2005) 4453–4464, https://doi.org/10.1021/ie058003d.
[28] D.L. Minnick, T. Turnaoglu, M.A. Rocha, M.B. Shiflett, Review Article: gas and vapor sorption measurements using electronic beam balances, J. Vac. Sci. Technol. 36 (2018), 050801, https://doi.org/10.1116/1.5044552.
[29] J. Crank, Diffusion in a plane sheet, in: The Mathematics of Diffusion, second ed., Oxford University Press, London, 1975, pp. 47–48.
[30] M.A. El-Okazy, L. Liu, C.P. Junk, E. Kathmann, W. White, S.E. Kentish, Gas separation performance of copolymers of perfluoro(butenyl vinyl ether) and perfluoro(2,2-dimethyl-1,3-dioxole), J. Membr. Sci. 634 (2021) 119401, https://doi.org/10.1016/j.memsci.2021.119401.
[31] S.M. Nemser, I.C. Roman, Perfluorodioxole Membranes, US5051114B2, 1990.
[32] S. Matteucci, Y. Yampolskii, B.D. Freeman, I. Pinnau, Transport of Gases and Vapors in Glassy and Rubbery Polymers, Materials Science of Membranes for Gas and Vapor Separation, 2006, pp. 1–47, https://doi.org/10.1002/047002903X.CH1.
[33] W.W.Y. Chow, K.F. Lei, G. Shi, W.J. Li, Q. Huang, Microfluidic channel fabrication by PDMS-interface bonding, Smart Mater. Struct. 15 (2005) 112–116, https://doi.org/10.1088/0964-1726/15/1/018.
[34] S.-H. Park, K.-J. Kim, W.-W. So, S.-J. Moon, S.-B. Lee, Gas separation properties of 6FDA-based polyimide membranes with a polar group, Macromol. Res. 11 (2003) 157–162, https://doi.org/10.1007/BF03218346.
[35] R.M. Lynden-Bell, E.L. Quitevis, The importance of polarizability: comparison of models of carbon disulphide in the ionic liquids $[C_1C_1im][NTf_2]$ and $[C_4C_1im][NTf_2]$, Phys. Chem. Chem. Phys. 18 (2016) 16535–16543, https://doi.org/10.1039/C6CP01752E.
[36] D.R. Paul, Dual Mode Sorption Model, Encyclopedia of Membranes, 2014, pp. 1–2, https://doi.org/10.1007/978-3-642-40872-4_662-3.
[37] L.M. Robeson, The upper bound revisited, J. Membr. Sci. 320 (2008) 390–400, https://doi.org/10.1016/J.MEMSCI.2008.04.030.